Journal of Zhejiang University-SCIENCE A (Applied Physics & Engineering)
ISSN 1673-565X (Print); ISSN 1862-1775 (Online)
www.zju.edu.cn/jzus; www.springerlink.com
E-mail: jzus@zju.edu.cn

A combined simulation of high speed train permanent magnet traction system using dynamic reluctance mesh model and Simulink*

Xiao-yan HUANG[1], Jian-cheng ZHANG[1], Chuan-ming SUN[2],
Zhang-wen HUANG[1], Qin-fen LU[†‡1], You-tong FANG[1], Li YAO[3]

([1]*School of Electrical Engineering, Zhejiang University, Hangzhou 310027, China*)

([2]*CSR Qingdao Sifang Co. Ltd., Qingdao 266111, China*)

([3]*Danfoss (Tianjin) Ltd., Tianjin 301700, China*)

[†]E-mail: luqinfen@zju.edu.cn

Received Sept. 22, 2014; Revision accepted Apr. 7, 2015; Crosschecked July 20, 2015

Abstract: This paper presents a combined dynamic parameter model (DPM) of a high speed train permanent magnet traction system using a dynamic reluctance mesh model and MATLAB Simulink. First, the dynamic reluctance model of the permanent magnet synchronous motor is introduced. Then the combined models of the traction system under i_d=0 and maximum torque per ampere control are built. Simulations using both constant parameter models and DPM models are carried out. The speed and torque characteristics are obtained. The results confirm that the DPM model provides higher accuracy without much sacrifice of time consumption or computation resource.

Key words: Permanent magnet traction system, Dynamic reluctance mesh model, Dynamic parameter model (DPM), High speed train, Maximum torque per ampere control

doi:10.1631/jzus.A1400284 **Document code:** A **CLC number:** TM922.71

1 Introduction

Permanent magnet (PM) motor traction systems for high speed railways have been highlighted recently due to their inherent advantages in terms of compact structure, high efficiency, and high power factor (Matsuoka, 2007). Some prototype trains have been independently developed by Alstom, Bombardier, and Siemens. Although large-scale commercial application is not in prospect at the moment, the PM motor traction system is considered as one of the most advanced high speed train technologies for the future (Mermet-Guyennet, 2010; Lee, 2012).

A common way to evaluate the performance of the PM motor traction system is a dynamic simulation using the MATLAB Simulink models (Lu *et al.*, 2011). However, the PM motor Simulink model is based on constant machine parameters such as resistance, *d*-axis inductance (L_d), *q*-axis inductance (L_q) but, in practice, the parameters such as L_d and L_q vary during operation. Therefore, the PM motor Simulink model cannot represent the real situation.

The finite element PM motor model can be used together with the Simulink power electronics model for accurate and complete solutions for detailed behavior (Ugalde *et al.*, 2009). However, a substantial amount of computational resources and much longer computational time are needed, especially for the traction motor which is normally rated at a few hundred kilowatts.

‡ Corresponding author

* Project supported by the National Natural Science Foundation of China (Nos. 51177144 and 51477149), the National High-Tech R&D Program (863 Program) of China (No. 2011AA11A101), the Qianjiang Talent Program (No. 2013R10031), and the Fundamental Research Funds for the Central Universities (No. 2014QNA4012), China

ORCID: Xiao-yan HUANG, http://orcid.org/0000-0001-5185-9040

The dynamic mesh modeling (DRM) method was developed by Carpenter (1968), Ostovic (1986; 1988; 1989), Sewell *et al.* (1999), and Yao (2006). It is based on the reluctance mesh. The magnetic field behavior is mapped onto an equivalent lumped equivalent circuit. This DRM method can save computation time without compromising accuracy (Dogan *et al.*, 2013; Araujo *et al.*, 2014; Nguyen-Xuan *et al.*, 2014). Therefore, in this paper, a dynamic mesh PM motor model is built and combined with Simulink power electronics models for better accuracy and higher simulation efficiency.

2 Dynamic reluctance mesh model

2.1 Principle of basic reluctance mesh (RM) model

The DRM method is based on the concept of equivalent magnetic circuits. Many laws and analysis methods for magnetic circuits can be analogous to those of electric circuit theory. In electric circuits, the fundamental parameters are voltage (V), current (I), and resistance (R_e), and their behavior is described by network constraints, such as Kirkhoff's voltage and current laws, and their constitutive relationships are described by, for example, Ohm's law. In magnetic circuits, the corresponding fundamental parameters are magnetomotive (MMF), flux (Φ), and reluctance (R_m) as shown in Table 1. A simplified RM motor model consists of nine components as shown in Fig. 1, where the square components represent the reluctance while the circle component represents the MMF.

Table 1 Fundamental parameters in magnetic and electric circuits

Magnetic circuit	Reluctance	MMF	Flux
	R_m	MMF=$\Phi \cdot R_m$	Φ=MMF/R_m
Electric circuit	Resistance	Voltage	Current
	R_e	$V=IR_e$	$I=V/R_e$

The magnetic circuit laws are analogous to those of electric circuits as follows: Kirkhoff's current and voltage law for magnetic circuits, for each node,

$$\sum_k \phi_k = 0, \tag{1}$$

$$\sum_k F_k = 0, \tag{2}$$

where ϕ_k is the flux and F_k is the MMF.

The reluctance of each component can be calculated by

$$R_m = \frac{l}{\mu A}, \tag{3}$$

where l is the length, A is the cross section area of each component, and μ is the permeability.

Based upon the above equations, the performance of the machine can be investigated.

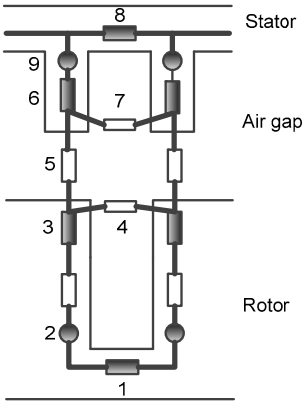

Fig. 1 Simplified RM model

1: rotor yoke; 2: magnetic source in rotor (permanent magnet); 3: rotor pole; 4: leakage between rotor poles; 5: air gap between stator and rotor; 6: stator teeth; 7: air gap between stator teeth; 8: stator yoke; 9: magnetic source in stator

2.2 Dynamic reluctance mesh model

The air gap plays a very important role in performance of the PM motor, because its reluctance is large compared to that of the other parts. Therefore, the air gap model is a key factor in simulating electrical machine performance accurately. However, air gap reluctances change as the rotor rotates, because under different rotor positions, the coupling between stator and rotor teeth is different.

In this study, the air gap reluctance is recalculated at every instantaneous rotor position. This is also the reason why the reluctance mesh is "dynamic". The torque can be calculated from the derivatives of the energy (co-energy) versus the displacement of the rotor. Since the air gap is the only parameter that

varies with the rotor position, the torque can be written as (Yao, 2006)

$$T_{\mathrm{e}}=\sum_{i=0}^{N-1}\left(\frac{1}{2}\frac{B_i^2 d_i l_i}{\mu_0}\frac{\partial w_i}{\partial\theta}\right), \tag{4}$$

where B_i is the flux density in the ith air gap reluctance, μ_0 is the permeability of the vacuum, θ is the angle, N is the turn number of the winding, and d_i, l_i, w_i are the depth, length, width of the ith air gap reluctance, respectively.

2.3 DRM model of the PM traction motor

A quarter model of the PM traction motor analyzed in this study is shown in Fig. 2. The interior PM rotor structure is used to improve the torque performance of the traction motor. However, due to the complex rotor structure, the magnetic calculation will be more challenging, especially in the calculation of L_d and L_q. Based on the analysis above, the reluctance network model per pole pair is built as shown in Fig. 3. In addition, the equivalent magnetic network model of the air gap at a certain rotor position is shown in Fig. 4, which should be changed as the rotor rotates as discussed above.

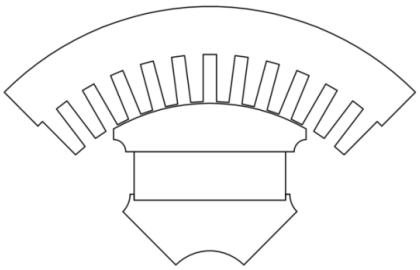

Fig. 2 Quarter model of the PM traction motor

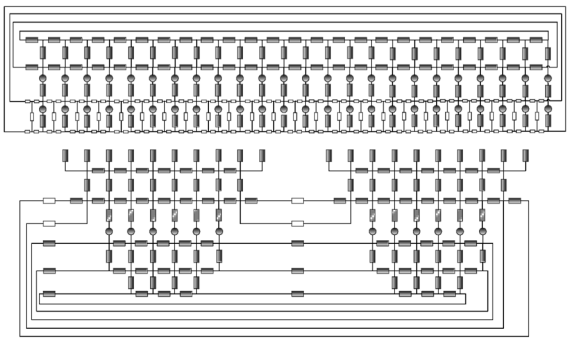

Fig. 3 Reluctance network model of the PM motor

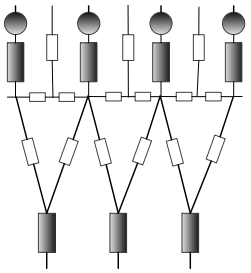

Fig. 4 Equivalent magnetic network model of the air gap

2.4 Simulation results of DRM model

Using the DRM model, the main motor parameters such as electromotive force (EMF) at no-load conditions, L_d and L_q can be accurately calculated in less time.

The back EMF at the no-load condition is calculated by Eq. (5). Based on the winding distribution, the phase-A winding is across a number k of stator teeth, so the flux linkage of phase-A winding can be expressed as Eq. (6). The comparison results for the back EMF separately calculated by DRM and finite element method (FEM) are presented in Fig. 5. It can be seen that the result calculated by DRM has a good agreement with that calculated by FEM.

$$E_A=-\frac{\mathrm{d}\Phi_A}{\mathrm{d}t}, \tag{5}$$

$$\Phi_A=\sum_{i=1}^{k}N\cdot\varphi_i, \tag{6}$$

where E_A is the back EMF at the no-load condition of phase-A winding, Φ_A is the flux linkage of phase-A winding, and φ_i is the flux through stator tooth i.

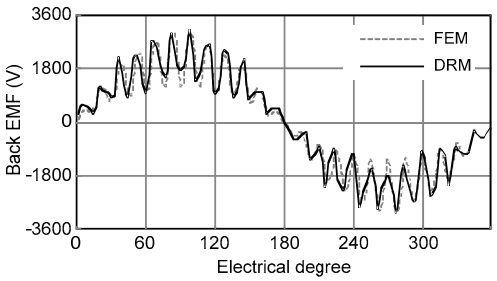

Fig. 5 Back EMF results calculated by DRM and FEM

As for calculation of L_d and L_q, an advanced method called frozen permeability is used to consider the effect of saturation caused by magnets and current.

The frozen permeability method calculates the inductance through two calculations. In the first calculation, excitation sources of both the winding current and the magnet are active. The resulting permeability distribution from the first calculation is used in the second calculation. In addition, in the second calculation, the magnet is set to inactive, so only the winding current is involved. Thus, the inductance can be calculated through Eq. (7). The inductance calculation results are presented in Fig. 6, and show good agreement with the FEM calculation.

$$L=\frac{\mathrm{d}\psi}{\mathrm{d}I}. \tag{7}$$

where L is the inductance, and ψ is the flux linkage.

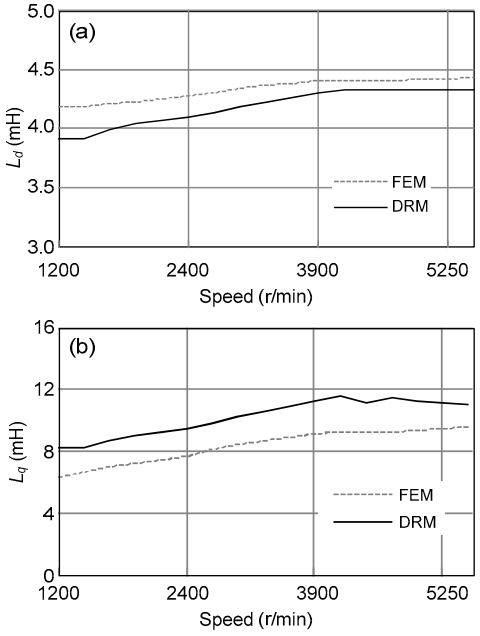

Fig. 6 L_d (a) and L_q (b) calculated by DRM and FEM

3 Combined model using DRM and Simulink

The basic concept of the combined Simulink-DRM simulation is using the DRM model as the motor model, while using the control system model provided by Simulink. There are two common ways to implement the combined Simulink-DRM simulation:

1. Replacing the DRM of PM motors for the constant parameter model (CPM) of PM motors provided by Simulink. DRM and Simulink will be running simultaneously. The dynamic parameters will be provided by DRM. However, for every time-stepping, the DRM and Simulink models need iteration calculation, which makes the simulation more complicated and time-consuming.

2. A dynamic parameters database is generated using DRM simulation. Then the dynamic parameters are put in the CPM in Simulink using the database index or lookup table. In this case the constant parameters in the traditional Simulink model will be modified instantaneously according to the motor operating condition. Compared to the first method, this method is more efficient without sacrifice of accuracy. Therefore, it will be adopted in this study.

The combined simulation carried out in this paper is based on the following assumptions:

1. Ignoring the effect of rotor skew on the stator back-EMF harmonics;

2. Keeping the excitation from the PM constant;

3. Ignoring the saturation of stator end winding flux leakage.

3.1 Dynamic modeling and interface

The dynamic parameter permanent magnet synchronous motor (PMSM) model was built using the Simulink S-function block, to replace the traditional CPM. The following equations are used with the S-function block to build the *d*-*q* coordinated PMSM model (Wang, 2011):

$$\begin{cases} u_d = R_1 i_d - \omega\psi_d + \dfrac{\mathrm{d}\psi_d}{\mathrm{d}t}, \\ u_q = R_1 i_q - \omega\psi_q + \dfrac{\mathrm{d}\psi_q}{\mathrm{d}t}, \end{cases} \tag{8}$$

$$\begin{cases} \psi_d = L_d i_d + \psi_\mathrm{m}, \\ \psi_q = L_q i_q, \end{cases} \tag{9}$$

$$\frac{\mathrm{d}\omega}{\mathrm{d}t}=\frac{1}{J}(T_\mathrm{e}-T_\mathrm{f}-F\omega-T_\mathrm{m}), \tag{10}$$

$$T_\mathrm{e}=\frac{3}{2}p[\psi_\mathrm{m} i_q+(L_d-L_q)i_d i_q], \tag{11}$$

where u_d, u_q are the voltage of the *d*-, *q*-axis; i_d, i_q are the current of the *d*-, *q*-axis; ψ_d, ψ_q, ψ_m are the flux linkage of the *d*-, *q*-axis, and permanent magnet flux linkage; T_e, T_f, T_m are the electric torque, friction torque, and load torque; J, F are the inertia, friction; L_d, L_q are the inductance of the *d*-, *q*-axis, respectively, and ω is the angular speed. In dynamic parameter models, L_d, L_q vary with the rotor position.

3.2 Vector control system

The basic concept of PMSM vector control is to control the PMSM like a separately excited DC motor. The stator current can be defined in the *d*-*q* coordinate system. The field flux linkage component of the current is normally aligned with the *d*-axis while the torque component of the current is aligned along the *q*-axis. By controlling i_d and i_q, the field and torque can be controlled respectively. In this study, the traction system behavior under i_d=0 and maximum torque per ampere control (MTPA) will be investigated.

1. PMSM with i_d=0 control

According to Eq. (11), when i_d=0, the torque will be determined by controlling i_q. In the case of i_d=0, there is no reluctance torque, which means it is more suitable for a non-saliency motor. In this study, the salient PMSM will be used. Thus, this method is not the best choice and is only be used here to provide comparison with other methods.

2. MTPA

For the MTPA control, the following equations are used (Tang, 1997):

$$\begin{cases} \dfrac{\partial(T_\mathrm{e}/i_\mathrm{s})}{\partial i_d}=0, \\ \dfrac{\partial(T_\mathrm{e}/i_\mathrm{s})}{\partial i_q}=0. \end{cases} \tag{12}$$

Keeping stator current i_s constant, and substituting $i_\mathrm{s}=\sqrt{i_d^2+i_q^2}$ into Eq. (12), i_d can be written as

$$i_d=\frac{-\psi_\mathrm{m}+\sqrt{\psi_\mathrm{m}^2+4(L_d-L_q)^2 i_q^2}}{2(L_d-L_q)}, \tag{13}$$

and then the torque can be rewritten as

$$T_\mathrm{e}=\frac{3}{4}pi_q\left(\sqrt{\psi_\mathrm{m}^2+4(L_d-L_q)^2 i_q^2}+\psi_\mathrm{m}\right). \tag{14}$$

For any given torque, the minimum i_d, i_q can be found.

3.3 Combine DRM and Simulink model

1. Traction system model with i_d=0

Fig. 7 shows the PMSM traction system diagram with i_d=0. The i_d reference is set to zero. i_q will be controlled by the proportional integral (PI) controlled according to the speed error. The PMSM model is built using an S-function and L_d, L_q vary with the rotor position.

2. Traction system model with MTPA

PMSM traction system with MTPA control is similar to that with the i_d=0 control. The only difference is that i_d, i_q will be calculated according to the torque demand using Eq. (14) as shown in Fig. 8. It can be seen from the equation that the torque and current relationship cannot be solved directly. In this study, an MTPA control block using the S-function will be built to determine i_q using a bi-section method for the numeric solution. Then i_d can be found.

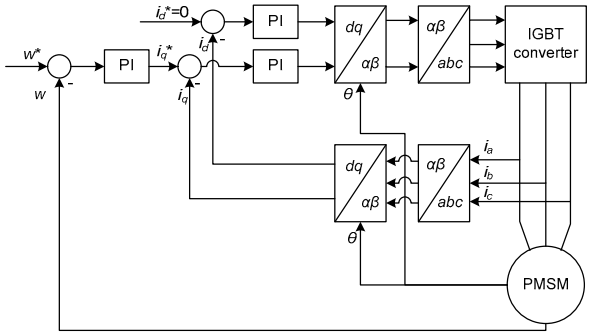

Fig. 7 PMSM traction system diagram with i_d=0

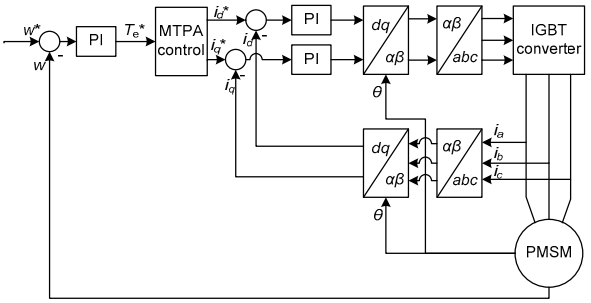

Fig. 8 PMSM traction system diagram with MTPA

4 Simulation results

A 600 kW PMSM traction system model for a high speed train was built. The required starting torque is 3500 N·m. In the constant torque area, the rated torque is 1350 N·m and the speed is 3000 r/min. In the brake mode, the speed will reduce to zero. The output current and torque were observed.

4.1 Constant parameter PMSM traction system Simulink models

The first model had i_d=0 using Simulink built in blocks. Both i_d=0 and MTPA control were adopted.

The motor dynamic speed response, torque, i_d, i_q, and power factor were compared under both control strategies, as shown in Fig. 9.

The speed response is faster and smoother under the MTPA control as shown in Fig. 9a. It also can be seen from Fig. 9b, under both control methods, that the output torque can be controlled precisely, providing starting and braking torque of 3500 N·m. However, with i_d=0 control, the torque pulsation was greater than that under MTPA control. It means that the system has better transient performance under MTPA control. For the phase-*A* current, as shown in Fig. 9c, for the same torque, with MTPA control the current is much less than with i_d=0 control, which will lead to high efficiency of the PMSM. i_d could be less than zero to realize field weakening control under MTPA control as shown in Figs. 9d and 9e. In this case, the operation speed range can be extended. The power factor with MTPA control was better as shown in Fig. 9f.

Based upon the above simulation results, it can be concluded that although the MTPA are more complicated, they have advantages in terms of fast transient behavior, high efficiency, and high power factor.

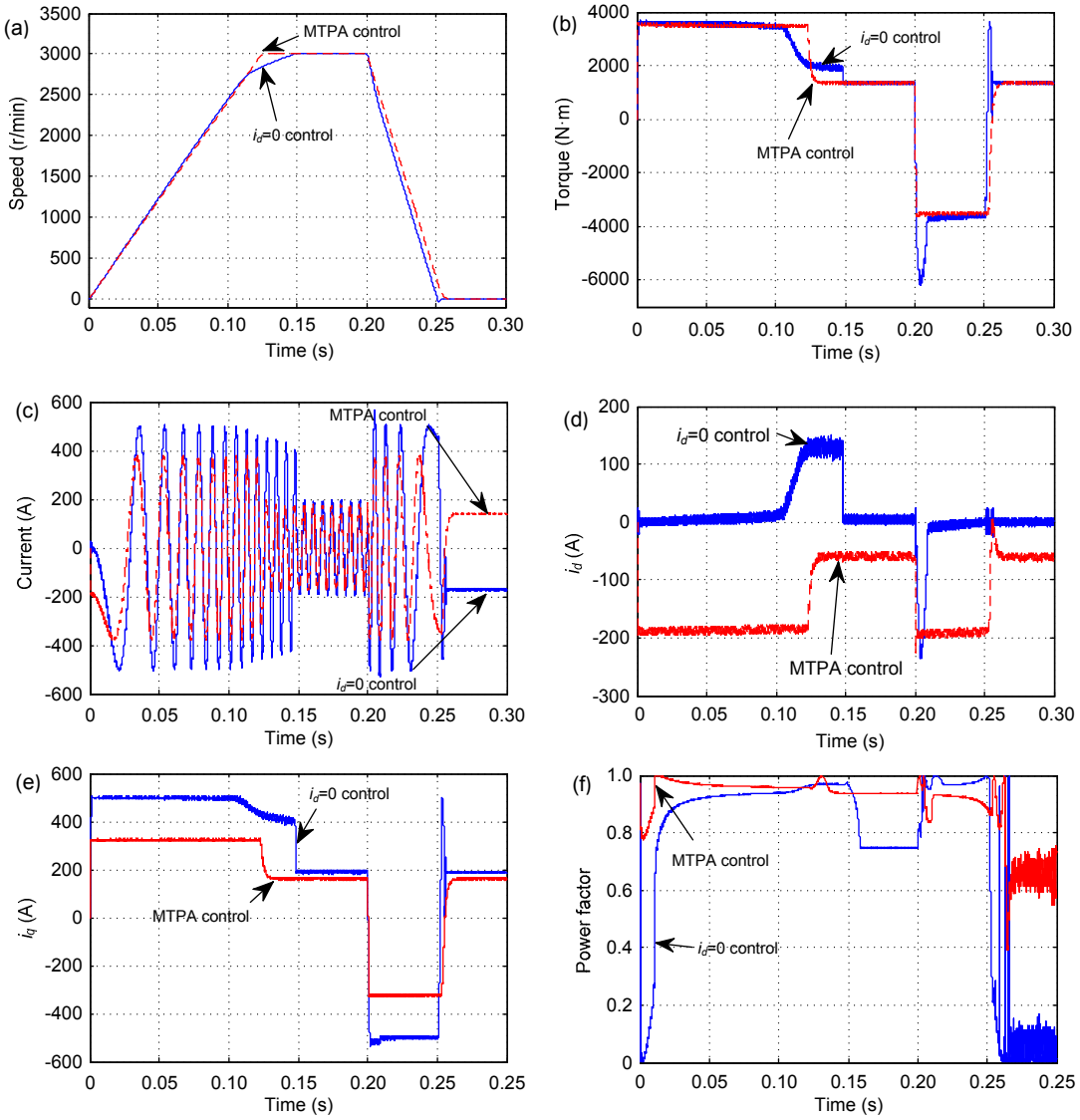

Fig. 9 Comparison of system behavior under i_d=0 and MTPA control using Simulink model
(a) Speed response; (b) Torque; (c) Phase-*A* current; (d) i_d; (e) i_q; (f) Power factor

4.2 Combined simulation using DRM and Simulink

The key feature of the combined simulation using DRM and Simulink is that L_d and L_q vary with the rotor position. However, the changes of L_d and L_q will not have much effect under i_d=0 control. Thus, the system performance under i_d=0 control will not be investigated in this study. The transient behavior using CPM and combined DPM under MTPA control will be compared. The simulations were carried out. The results are shown in Fig. 10.

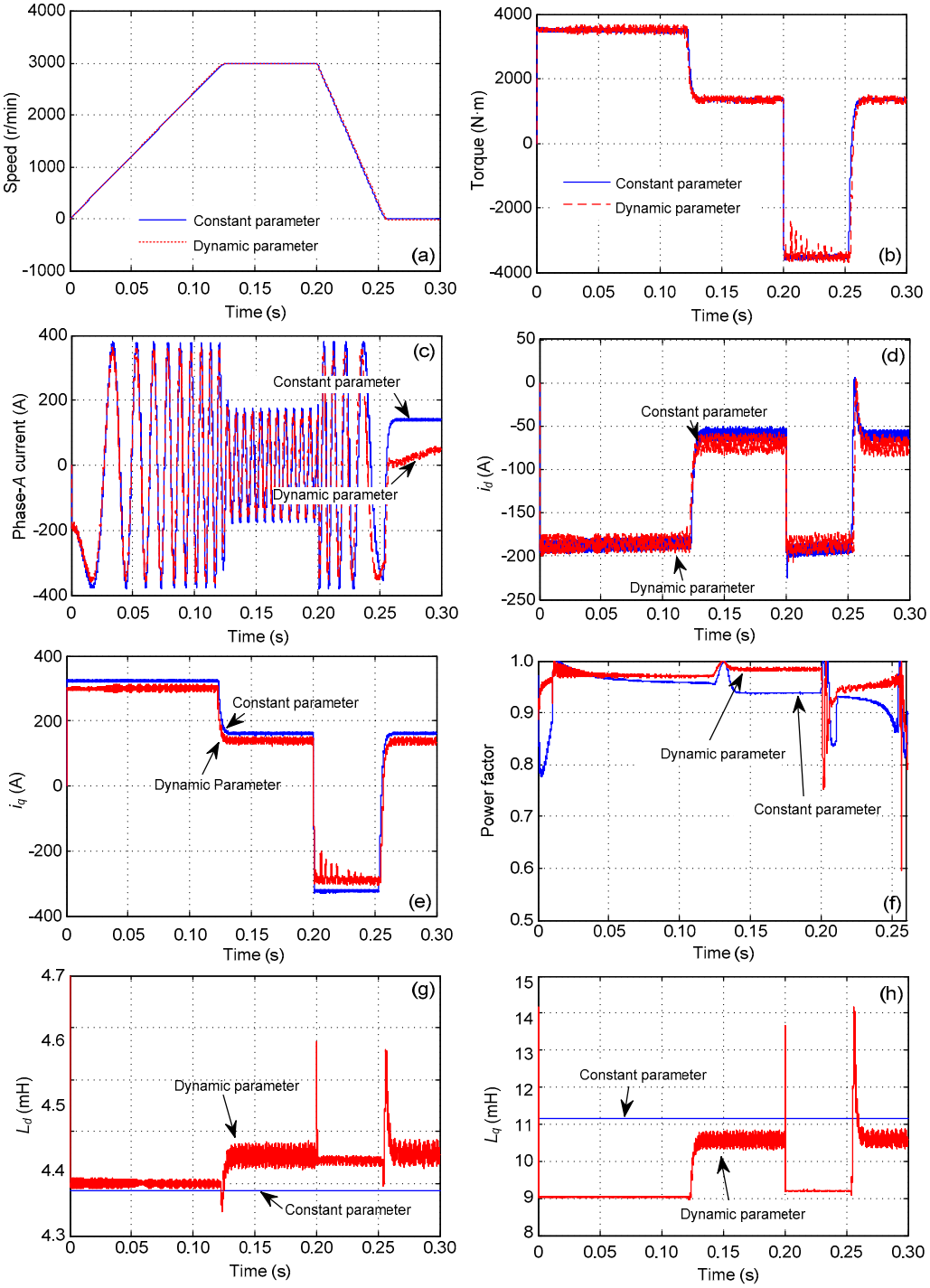

Fig. 10 Comparison of simulations using constant parameter model and dynamic parameters model under MTPA control
(a) Speed response; (b) Torque; (c) Phase current; (d) i_d; (e) i_q; (f) Power factor; (g) L_d; (h) L_q

The transient behavior of the system under each model is similar except for the L_d and L_q as shown in Fig. 10. However, during the acceleration of the train, the system was operating in the constant torque area, and the output torque waveform is as shown in Fig. 11. Because of the variation of i_d and i_q, the degree of motor saturation varied and therefore L_d and L_q varied. The output torque varied accordingly, especially when the speed was further increased, and the torque pulsation increased correspondingly.

During the braking operation, the output torque waveforms using the CPM and DPM are shown in Fig. 12. The system was in the field weakening operation, therefore L_d and L_q varied dramatically due to saturation, which leads to a large torque pulsation.

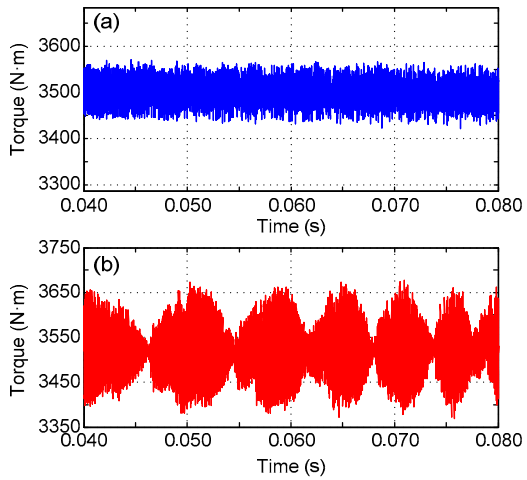

Fig. 11 Output torque under speed accelerating operation: (a) CPM; (b) DPM

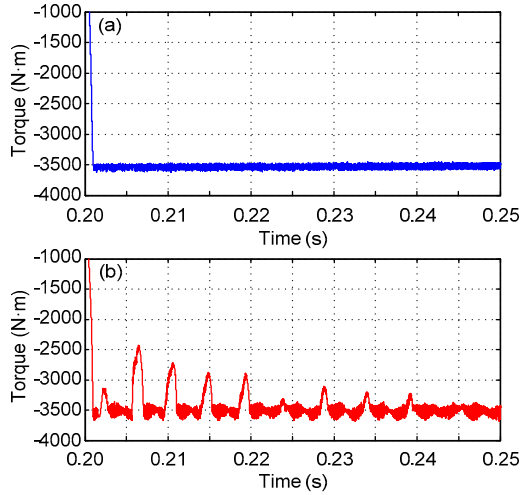

Fig. 12 Comparison of output torque during the braking operation: (a) CPM; (b) DPM

5 Conclusions

This paper presented a combined dynamic parameter PMSM traction system model using the DRM and MATLAB-Simulink. Models under i_d=0 and MTPA control were built. Simulations were carried out under real high speed train operation including acceleration, constant speed, and braking. The results proved that the system with MTPA control has advantages in terms of fast transient response, and high power factor and efficiency. Simulations using both CPM and DPM models were carried out. The results confirm that the DPM model provides higher accuracy without much sacrifice of time consumption or computation resource. The combined DPM model was shown to be useful and able to provide a reference for the actual design and production of a high speed train traction system.

References

Araujo, D.M., Coulomb, J.L., Chadebec, O., *et al.*, 2014. A hybrid boundary element method-reluctance network method for open boundary 3-d nonlinear problems. *IEEE Transactions on Magnetics*, **50**(2):77-80. [doi:10.1109/TMAG.2013.2281759]

Carpenter, C.J., 1968. Magnetic equivalent circuits. *Proceedings of the Institution of Electrical Engineers*, **115**(10):1503-1511.

Dogan, H., Garbuio, L., Nguyen-Xuan, H., *et al.*, 2013. Multistatic reluctance network modeling for the design of permanent-magnet synchronous machines. *IEEE Transactions on Magnetics*, **49**(5):2347-2350. [doi:10.1109/TMAG.2013.2243426]

Lee, K.K., 2012. The evolution and outlook of core technologies for high-speed railway in China. 1st International Workshop on High-speed and Intercity Railways, **2**:495-507. [doi:10.1007/978-3-642-27963-8_45]

Lu, Q.F., Wang, B., Huang, X.Y., *et al.*, 2011. Simulation software for CRH2 and CRH3 traction driver systems based on Simulink and VC. *Journal of Zhejiang University-SCIENCE A (Applied Physics & Engineering)*, **12**(12):945-949. [doi:10.1631/jzus.A11GT006]

Matsuoka, K., 2007. Development trend of the permanent magnet synchronous motor for railway traction. *IEEJ Transactions on Electrical and Electronic Engineering*, **2**(2):154-161. [doi:10.1002/tee.20121]

Mermet-Guyennet, M., 2010. New power technologies for traction drives. International Symposium on Power Electronics, Electrical Drives, Automation and Motion, Pisa, Italy, p.719-723.

Nguyen-Xuan, H., Dogan, H., Perez, S., *et al.*, 2014. Efficient reluctance network formulation for electrical machine

design using optimization. *IEEE Transactions on Magnetics*, **50**(2):869-872. [doi:10.1109/TMAG.2013.2282407]

Ostovic, V., 1986. A method for evaluation of transient and steady state performance in saturated squirrel cage induction machines. *IEEE Transactions on Energy Conversion*, **1**(3):190-197.

Ostovic, V., 1988. A simplified approach to magnetic equivalent-circuit modeling of induction machines. *IEEE Transactions on Industry Applications*, **24**(2):308-316.

Ostovic, V., 1989. A novel method for evaluation of transient states in saturated electric machines. *IEEE Transactions on Industry Applications*, **25**(1):96-100.

Sewell, P., Bradley, K.J., Clare, J.C., *et al.*, 1999. Efficient dynamic models for induction machines. *International Journal of Numerical Modelling: Electronic networks, devices and fields*, **12**(6):449-464. [doi:10.1002/(sici)1099-1204(199911/12)12:6<449::aid-jnm365>3.0.co;2-w]

Tang, R.Y., 1997. Modern Permanent Magnet Machines: Theory and Design. China Machine Press, Beijing, China, p.473 (in Chinese).

Ugalde, G., Almandoz, G., Poza, J., *et al.*, 2009. Computation of iron losses in permanent magnet machines by multi-domain simulations. 13th European Conference on Power Electronics and Applications, Barcelona, p.1-10.

Wang, X.H., 2011. Permanent Magnet Machines. China Electric Power Press, Beijing, China, p.327 (in Chinese).

Yao, L., 2006. Magnetic Field Modelling of Machine and Multiple Machine Systems Using Dynamic Reluctance Mesh Modelling. PhD Thesis, University of Nottingham, Nottingham, UK.

中文概要

题　目: 基于动态磁网络和 Simulink 的高速铁路牵引传动系统联合仿真

目　的: 提出基于动态磁网络和 Simulink 的高速铁路牵引传动系统的动态参数模型，提高高速铁路牵引传动系统仿真分析的准确度。

方　法: 将动态磁网络计算得出的动态参数 L_d，L_q 等以查表的形式嵌入 Simulink 模型，有效地实现动态参数。

结　论: 该动态参数模型能在不显著增加仿真运算量和仿真时间的条件下有效地提高计算的准确度。

关键词: 高速铁路牵引传动系统；永磁电机；动态参数模型；动态磁网络；Simulink